

# Propagation of crackle-containing jet noise from high-performance engines

Kent L. Gee<sup>a)</sup>, Tracianne B. Neilsen<sup>b)</sup>, Alan T. Wall<sup>c)</sup>, J. Micah Downing<sup>d)</sup>,  
Michael M. James<sup>e)</sup> and Richard L. McKinley<sup>f)</sup>

(Received: 16 July 2015; Revised: 17 December 2015; Accepted: 18 December 2015)

**Crackle, the impulsive quality sometimes present in supersonic jet noise, has traditionally been defined in terms of the pressure waveform skewness. However, recent work has shown that the pressure waveform time derivative is a better quantifier of the acoustic shocks believed to be responsible for crackle perception. This paper discusses two definitions of crackle: waveform asymmetry versus shock content and crackle as a source or propagation-related phenomenon. Data from two static military jet aircraft tests are used to demonstrate that the skewed waveforms radiated from the jet undergo significant nonlinear steepening and shock formation, as evidenced by the skewness of the time derivative of the pressure waveforms. To the extent that crackle is caused by the presence of shock-like features in the waveform, crackle's perceived quality is likely to be heavily influenced by propagation through the geometric near field and into the far field. © 2016 Institute of Noise Control Engineering.**

Primary subject classification: 13.1.2; Secondary subject classification: 21.6.1

## 1 INTRODUCTION

Crackle, a supersonic jet noise phenomenon, has been labeled as an annoying and dominant characteristic of the total noise<sup>1,2</sup> and is, therefore, an important consideration when designing noise reduction methodologies for tactical aircraft. Ffowcs Williams et al.<sup>1</sup> described crackle as “sudden spasmodic bursts of a rasping fricative sound . . . It is a startling staccato of cracks and bangs and its onomatopoe, ‘crackle,’ conveys a subjectively accurate impression.” A principal conclusion by Ffowcs Williams et al. was that the skewness of the pressure waveform,  $Sk\{p(t)\}$ , a normalized third central moment of the waveform probability

density function (PDF) and measure of the PDF asymmetry, can be used to conveniently identify a crackling jet.

The work of Ffowcs Williams et al. has guided subsequent supersonic jet noise investigations. Shortly after the Ffowcs Williams et al. study was published, Schlinker<sup>3</sup> reported skewness values in his dissertation on laboratory-scale supersonic jet experiments. More recently, several studies have included  $Sk\{p(t)\}$  as part of laboratory and full-scale experiment documentation and discussed implications regarding crackle<sup>2,4–14</sup>. Crighton<sup>13</sup> sought an explanation for pressure skewness in the context of atmospheric nonlinear propagation of jet noise, a theme that has been discussed more recently by Petitjean and McLaughlin<sup>5</sup>, Petitjean et al.<sup>6</sup> and Schlinker et al.<sup>10,11</sup>. Source mechanisms for an asymmetric pressure PDF have also been sought. Krothapalli et al.<sup>2</sup> described pressure skewness as a source mechanism resulting from Mach wave radiation and proposed that asymmetric waveforms were caused by pockets of rapidly expanding cool, ambient air when entrained in a hot jet.

A possible connection between jet Mach wave radiation and crackle/skewness has been described by other authors, including the potential for crackle reduction<sup>7,8,14</sup>. Recent supersonic flow numerical simulations by Nichols et al.<sup>15,16</sup>, Anderson and Freund<sup>17</sup>, and Buchta et al.<sup>18</sup> have indicated that pressure skewness originates as a source phenomenon. Schlinker et al.<sup>10</sup> applied an eduction method to high-power set point data from a full-scale engine and localized the origin of impulsive signatures to be around 5 nozzle diameters downstream of the nozzle exit. Note further that positive pressure skewness associated with supersonic jet flows has been documented in military jet flyover data<sup>12,19</sup>,

<sup>a)</sup> Department of Physics and Astronomy, N283 ESC, Brigham Young University, Provo, UT 84602, USA; email: kentgee@byu.edu.

<sup>b)</sup> Department of Physics and Astronomy, N283 ESC, Brigham Young University, Provo, UT 84602, USA; email: tbn@byu.edu.

<sup>c)</sup> Department of Physics and Astronomy, N283 ESC, Brigham Young University, Provo, UT 84602, USA; email: alantwall@gmail.com.

<sup>d)</sup> Blue Ridge Research and Consulting, LLC, 29 N Market St #700, Asheville, NC 28801, USA; email: micah.downing@blueridgeresearch.com.

<sup>e)</sup> Blue Ridge Research and Consulting, LLC, 29 N Market St #700, Asheville, NC 28801, USA; email: michael.james@blueridgeresearch.com.

<sup>f)</sup> Battlespace Acoustics Branch, AFRL 711 HPW/RHCB, Air Force Research Laboratory, Wright-Patterson Air Force Base, OH, 45433, USA; email: richard.mckinley.1@us.af.mil.

in static rocket motors and launch vehicles<sup>20,21</sup>, and in explosive volcanic eruptions<sup>22</sup>.

Ffowcs Williams et al. are responsible for the synonymy of crackle with positive pressure skewness, but also indicated that the “physical feature of a sound wave that gives rise to the readily identifiable subjective impression of ‘crackle’ is shown to be the sharp shock-like compressive waves that sometimes occur in the wave form”. As pointed out by Papamoschou and Debiasi<sup>4</sup>, who called pressure skewness an “incomplete metric” for crackle, these two views are not necessarily compatible. Because  $\text{Sk}\{p(t)\}$  quantifies only the asymmetric occurrence of pressure values, it is wholly insensitive to large temporal rate of pressure changes,  $\partial p/\partial t$ , that define acoustic shocks. Gee et al.<sup>23</sup> have shown that the shock-like features present in a pressure waveform from an afterburning F/A-18E are essential in reproducing its crackle and suggested that the quantification of crackle should be based on statistics of the waveform time derivative. However, given its historical precedence and the fact that supersonic jets produce positively skewed waveforms, the use of  $\text{Sk}\{p(t)\}$  to describe jet crackle remains common today.

The cumulative body of work regarding jet crackle has included noise from heated and unheated, ideally and non-ideally expanded, and laboratory and full-scale jets. However, there has not been a consistent methodology nor framework for investigating the phenomenon, which may contribute to differing viewpoints regarding its origin. Ultimately, the issues raised by authors of prior jet crackle-related studies lead to this paper's principal question: how are the definitions of crackle based on (1) the waveform's PDF asymmetry and (2) the shock content phenomenologically different when analyzing data from high-performance military jet aircraft? The answer to this question impacts the design of noise reduction solutions to eventually reduce crackle as a perceptual phenomenon. To contextualize our physical approach to identifying a consistent definition for crackle, we first summarize research regarding the quantifying of acoustic shocks. Next, we describe and analyze two static full-scale experiments involving the F-35 AA-1 Lightning II and F-22A Raptor from the perspective of the two current definitions for jet crackle. As part of these analyses, we consider the effect of sampling rate on quantifying crackle. We note that, although the analyses are specific to the datasets here, particularly because jet operating conditions are not known, phenomenological connections to laboratory-scale datasets can be made.

## 2 QUANTIFYING ACOUSTIC SHOCKS

One of the attractive features of the study by Ffowcs Williams et al.<sup>1</sup> is that their definition of crackle was simple: waveforms for which  $\text{Sk}\{p(t)\} > 0.4$  distinctly crackled and waveforms for which  $\text{Sk}\{p(t)\} < 0.3$  did not

crackle. One issue with using  $\text{Sk}\{p(t)\} > 0.4$  as an absolute threshold for crackle is that the statistics of the waveform are dependent on the response of the data acquisition system. Ffowcs Williams et al. noted, “The skewness factors measured are likely therefore to be unique to this type of measurement and analysis equipment, which is in wide use throughout the international aviation community”<sup>1</sup>). Formulation of an acoustic shock-based description of crackle requires more background. In this paper, we use the skewness of the time derivative of the pressure,  $\text{Sk}\{\partial p/\partial t\}$ , hereafter referred to as derivative skewness, to examine the behavior of the shock-based definition of crackle. Other descriptors are possible: acoustic shocks in broadband noise have been analyzed based on instantaneous loudness<sup>24</sup> and wavelets<sup>25</sup>. Comparisons between different potential quantifiers of crackle will be the subject of future work.

The use of  $\text{Sk}\{\partial p/\partial t\}$  to quantify shock-like content originated with McNerny, who with others analyzed launch vehicle<sup>21</sup> and military jet data<sup>12,26</sup>. Since the demonstration<sup>23</sup> that the presence of large time derivatives in the waveform was important to representing crackle, the statistics of the pressure time derivative have been documented in various laboratory-scale experiments<sup>8,9,27–29</sup>. The derivative skewness is written for a zero-mean derivative process as

$$\text{Sk}\left\{\frac{\partial p}{\partial t}\right\} = \frac{\left\langle\left(\frac{\partial p}{\partial t}\right)^3\right\rangle}{\left\langle\left(\frac{\partial p}{\partial t}\right)^2\right\rangle^{3/2}}, \quad (1)$$

where  $\langle \cdot \rangle$  signifies ensemble average. Only recently have efforts been made to quantify its behavior relative to nonlinear acoustic shock formation and propagation. Shepherd et al.<sup>30</sup> considered the change in waveform and derivative statistics for lossless nonlinear propagation of an initial sinusoid, the derivative skewness of which is zero. They found a rapid increase in derivative skewness as  $\sigma \rightarrow 1$ , where  $\sigma$  is defined as the propagation distance relative to shock formation. A full analytical treatment of the same scenario<sup>31,32</sup> revealed that, for  $\sigma \ll 1$ , the derivative skewness could be approximated as a linear function,  $\text{Sk}\{\partial p/\partial t\} \approx 3\sigma/\sqrt{2}$ , whereas  $\text{Sk}\{\partial p/\partial t\} \approx (1 - \sigma^2)^{-3/4}$  as  $\sigma \rightarrow 1$ . This latter

<sup>1</sup>) Although they added a footnote in which they indicated they reproduced the results for many of their experiments using a recorder with a flatter low-frequency response, a rigorous evaluation of the threshold has not taken place. McNerny et al.<sup>21</sup>, in their studies of launch vehicle noise, showed that a loss of low-frequency response resulted in artificially greater skewness values, thereby affirming the potential problem in using the  $\text{Sk}\{p(t)\} > 0.4$  as an absolute threshold to define crackle for data acquired using modern instrumentation with different frequency responses.

expression yields a value of infinity at  $\sigma = 1$  as the initial slope discontinuity occurs in the waveform. Discrete temporal sampling of acoustic pressure data will necessarily limit the derivative skewness to finite values, but Reichman et al.<sup>31</sup> have shown that  $\text{Sk}\{\partial p/\partial t\} \approx 5$  indicates significant shock formation, provided that the sampling-to-peak-frequency ratio,  $f_s/f_{\text{peak}}$ , is at least 100.

These analytical investigations provide improved understanding of quantifying time-domain nonlinearity with the derivative skewness, but the acoustic radiation from a jet is nonplanar, nonsinusoidal, and within the geometric near field, noncompact. As Ffowcs Williams et al.<sup>1</sup> noted, geometric spreading by itself does not change the nature of the nonlinear propagation, just the distance at which shocks will occur. Muhlestein and Gee<sup>33</sup> experimentally confirmed the rapid growth of  $\text{Sk}\{\partial p/\partial t\}$  during shock formation of sinusoids in a plane-wave tube. They also showed that nonlinearly propagating broadband noise forms shocks relatively more quickly than an initial sinusoid of the same rms amplitude, leading to a more rapid increase in derivative skewness values. This more rapid increase is caused by the fact that, relative to the sinusoid, noise has larger pressure values and derivatives for waveforms of the same standard deviation. Reichman et al.<sup>31</sup> have further shown that the suggested threshold of  $\text{Sk}\{\partial p/\partial t\} > 5$  for significant shock formation is also applicable to the noise case studied by Muhlestein and Gee<sup>33</sup>.

For jets, the noncompact noise source region may result in geometric near-field nonlinear interactions<sup>29</sup>, thereby complicating the analysis. Nevertheless, if shocks are significantly present in a jet noise waveform, Eqn. (1) will yield large derivative skewness values regardless of the precise nature of the propagation or its location relative to the source. Conversely, small values of the derivative skewness indicate that shocks are not significantly present in the pressure waveform.

### 3 FULL-SCALE EXPERIMENT SUMMARIES

#### 3.1 F-35 AA-1 Lightning II

The F-35 AA-1 static run-up measurements were conducted on 18th of October 2008 at Edwards Air Force Base (EAFB), CA, by the Air Force Research Laboratory, Blue Ridge Research and Consulting, LLC and Brigham Young University. Photographs of the tied-down aircraft are displayed in Fig. 1. Measurements<sup>34–36</sup> were made using 6.35 mm Type 1 free-field and pressure microphones located at a height of 1.5 m (5 ft). The pressure microphones were oriented skyward, for nominally grazing incidence. The free-field microphones were pointed toward the plume, aimed at a jet centerline location approximately 6.7 m aft of the aircraft. This location, which is about 7–8 nozzle diameters downstream of the engine nozzle exit plane (the



Fig. 1—Tied-down F-35 AA-1 aircraft, with a portion of the geometric near-field microphone array.

same scaled distance used for a previous F-22A experiment in 2004)<sup>37</sup>, was set as the origin for defining observation angles. During the overall test, which consisted of 4–5 run-ups for each engine condition, the average wind speed was less than 1 kt and the ambient pressure was virtually constant at 0.914 kPa. Temperature and relative humidity varied from 7 to 16 °C and 21 to 27%, respectively. These meteorological data are given for completeness and the variations do not impact the measurements within the propagation range considered here. The results presented in Sec. 4 are for a single set of run-ups, but are consistent over the entire test: the spatially averaged standard deviation in overall sound pressure level (OASPL) across run-ups is less than 1 dB for all engine conditions.

The data analyzed here were obtained from a microphone array described previously<sup>34</sup> as a near-field array because it comprised locations out to 38 m from the origin. The geometric near and far fields are ill-defined for a supersonic jet, as the source peak location, extent and directivity vary with frequency, but a prior analysis<sup>29</sup> of OASPL decay for an unheated Mach 3.0 jet suggests that a transition to spherical spreading is complete by about 50 nozzle diameters. Data acquisition was carried out using a National Instruments® 8353 RAID server containing PXI-4462 cards. Analog input ranges for each channel were adjusted (in 10 dB increments) for low and high-power settings, based on the sensitivity of each microphone, in order to maximize the dynamic range of each 24-bit channel. The system sampling frequency was varied between 96 and 204.8 kHz. The lower sampling rate was required

because of slower mechanical hard drive write speeds for the early-morning tests while the system was cold and during afterburner, for which system vibration was greater. The system was located forward of the aircraft and to the sideline (about  $70^\circ$ ) at an approximate distance of 35 m. To illustrate the ranges of conditions, data at 50% engine thrust request (ETR) and 150% ETR (maximum afterburner power), both sampled at 96 kHz, are described in this paper. Additional, and complementary, results from these measurements are shown in Refs. 34–36 and 38–40. Reference 38 examines measurement crest factor, Ref. 39 describes the role of nonlinear propagation in the spectral shape and Ref. 40 compares two time-domain nonlinearity measures across the full range of engine conditions. Some of the results in Ref. 40 are also included here as they are relevant to the discussion of crackle

### 3.2 F-22A Raptor

In July 2009, Brigham Young University and Blue Ridge Research and Consulting, LLC, took extensive noise measurements near an F-22A Raptor at Holloman Air Force Base. The aircraft was tied down to a concrete run-up pad and one engine was cycled through idle, intermediate, military and afterburner while the other was held at idle. Pressure waveform data from 150 channels were acquired with a similar National Instruments-based recording system using PXI-446x and 449x series cards at 96 kHz for the three lower power conditions and 48 kHz at afterburner, because of slow mechanical hard drive write speeds caused by system vibration. A complete description of the experiment is found in Ref. 41.

The data analyzed in this study were recorded on a rectangular array of microphones placed near the aircraft, as shown in Fig. 2. The 90 microphones were located 15.2 cm (6.0 in) apart and covered an aperture 0.6 m high by 2.6 m (2 ft  $\times$  8.5 ft) long. The rig that held the microphones was positioned at ten locations and three heights



Fig. 2—The tied-down F22A Raptor with one engine at afterburner. Shown also is the 90-microphone rectangular array.

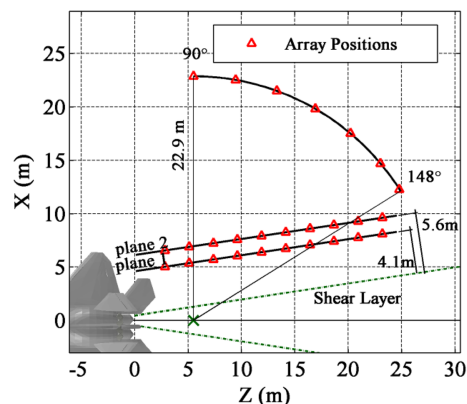


Fig. 3—Diagram of the experimental set-up for the acoustical measurements on an F-22A Raptor. The triangles, each 2.3 m apart, mark the center of the microphone array for individual scans. The “x” located 5.5 m downstream of the nozzle exit refers to the estimated peak source location and the angle measurement reference.

along a 22.9 m (75 ft)-long track and overlapped to form 1.8 m  $\times$  23.2 m (6 ft by 76 ft) measurement planes, as shown in Fig. 3. The triangles indicate the locations of the center of the microphone array at each measurement position. The set of measurements obtained 4.1 m from the shear layer of the jet plume is referred to as plane 1, while plane 2 refers to measurements taken 5.6 m from the shear layer of the jet plume. Additionally, measurements were taken in  $10^\circ$  increments along a 23 m arc referenced from the estimated peak source location<sup>37</sup>. The height of the array center was 1.9 m (75 in) for the arc measurements.

The data from this test are not as spatially diverse as the F-35 AA-1 measurements but are analyzed for three reasons. First, the aperture is sufficiently large to examine the data for spatial trends. Second, these data have previously been analyzed from a number of contexts, including level-based<sup>41</sup>, similarity spectra<sup>42</sup>, correlation<sup>43</sup> and intensity<sup>44</sup> analyses, to near-field acoustical holography<sup>45</sup> and equivalent source modeling<sup>46</sup>. Their inclusion here helps to add to the overall in-depth near-field characterization performed. Third, they are used to illustrate the deleterious effects of sampling frequency limitations on  $Sk\{\partial p/\partial t\}$ , which may be especially problematic for laboratory-scale testing. Note further that far-field nonlinear propagation analysis from prior 2004 F-22A measurements<sup>37</sup>, which covered a range of 23–305 m, is also germane to the discussion of crackle and acoustic shock formation.

## 4 F-35 AA-1 DATA ANALYSIS

The present F-35 AA-1 analysis builds on a previous limited investigation<sup>34</sup> and incorporates elements of a separate nonlinearity analysis<sup>40</sup> into the discussion on crackle.

We consider analyses of OASPL,  $Sk\{p(t)\}$  and  $Sk\{\partial p/\partial t\}$  for 50% ETR and 150% ETR in order to provide examples of low and high-power engine conditions. The three measures are shown in Fig. 4 for 50% ETR and Fig. 5 for 150% ETR. Between data at the marked microphone locations, a regularized bicubic interpolation<sup>47</sup> between data points reduces interpolation artifacts present in previous related studies. Although we recognize that the non-physical nature of the interpolation may result in reduced accuracy in sparse measurement regions or near the aircraft where significant shielding/scattering is expected, the maps provide a convenient means to visualize data trends across measurement positions.

The OASPL map in Fig. 4(a) for 50% ETR provides context for examining similar maps for skewness. The OASPL maximum at 38 m occurs near, but at angle

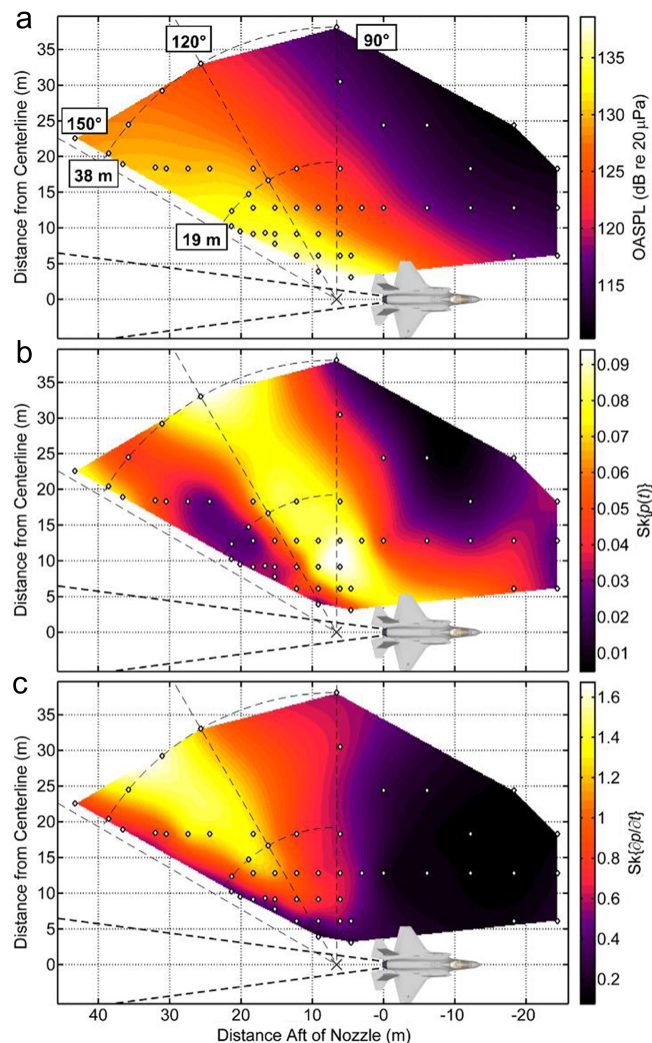


Fig. 4—Measurement of (a) OASPL, (b)  $Sk\{p(t)\}$  and (c)  $Sk\{\partial p/\partial t\}$  for the F-35 AA-1 at 50% ETR. The dashed lines from the nozzle indicate the approximate shear layer location.

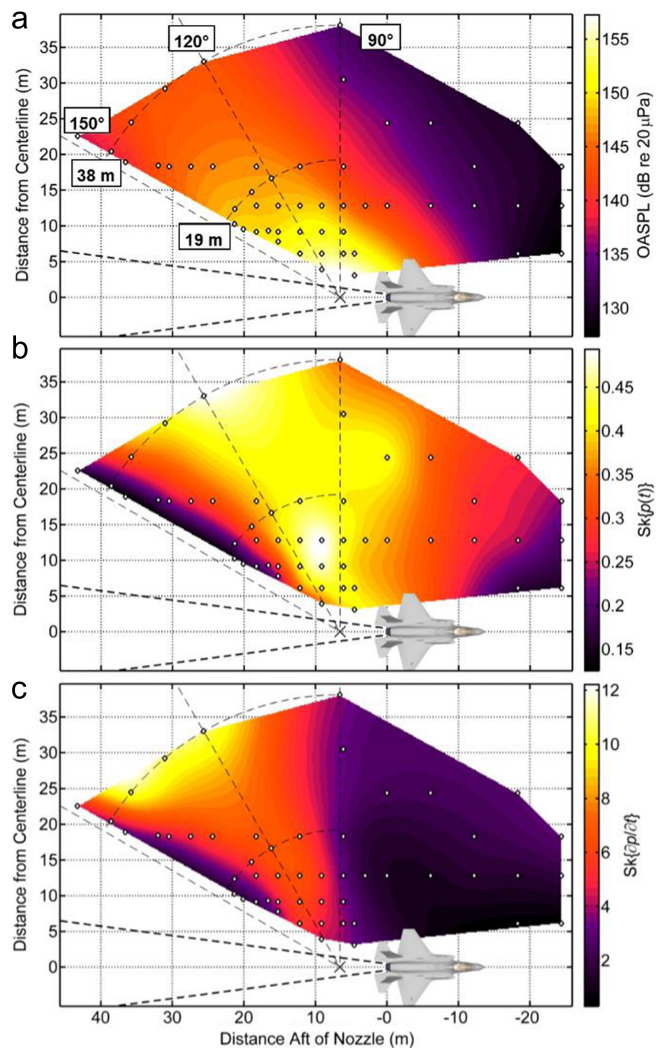


Fig. 5—Measurement of (a) OASPL, (b)  $Sk\{p(t)\}$  and (c)  $Sk\{\partial p/\partial t\}$  for the F-35 AA-1 at 150% ETR.

perhaps greater than,  $150^\circ$ , as defined relative to the engine inlet and the 6.7 m origin. Comparison of this maximum OASPL lobe with the pressure and derivative skewness maps, displayed in Figs. 4(b) and 4(c), respectively, reveals different trends for the two measures. In Fig. 4(b), the pressure skewness, though small ( $Sk\{p(t)\} < 0.1$ ), possesses a clear directivity whose maximum is approximately  $25^\circ$  upstream of the maximum OASPL lobe for this condition. The relative constancy of the pressure skewness (0.075–0.095) in the maximum direction outside the first few nozzle diameters provides evidence that  $Sk\{p(t)\}$  is produced as a source phenomenon, or at least very near the shear layer. On the other hand,  $Sk\{\partial p/\partial t\}$  in Fig. 4(c) exhibits fundamentally different behavior than  $Sk\{p(t)\}$ ; there is a clear trend in terms of increasing skewness of  $\partial p/\partial t$ , with larger magnitudes of the derivative occurring at greater distances from the source and  $\sim 15^\circ$  closer to the maximum OASPL lobe. The only known cause for a systematic increase in positive derivative magnitudes near the maximum

radiation direction is nonlinear waveform steepening. In this case, a maximum value of 1.62 near the shear layer when combined with the discussion in Sec. 2 indicates nonlinear waveform steepening, but not shock formation. This is confirmed by examining waveform segments at 4.6 and 38 m in Ref. 40. We note that the increasing  $Sk\{\partial p/\partial t\}$  with propagation distance agrees with findings from anechoic, laboratory-scale measurements of unheated<sup>9</sup> and heated<sup>8</sup> supersonic jets.

The OASPL,  $Sk\{p(t)\}$  and  $Sk\{\partial p/\partial t\}$  for maximum afterburner (150% ETR) are displayed in Fig. 5. Note that many of the same trends from 50% ETR are repeated, but with significantly greater values. The increase in thrust has shifted the main OASPL lobe in Fig. 5(a) toward the sideline, to approximately 125°. The values for  $Sk\{p(t)\}$  in Fig. 5(b) have increased significantly from 50% ETR, with values in excess of 0.35 over a very large angular aperture from about 80–140°. In addition,  $Sk\{p(t)\}$  appears to originate relatively close to the nozzle, potentially corroborating the 5 nozzle diameter estimate by Schlinker et al.<sup>10</sup>, although their full-scale engine measurements were made for a non-afterburning condition. The rapid decrease in  $Sk\{p(t)\}$  with increasing downstream distance along the aft edge of the measurement aperture agrees with laboratory-scale measurements by Mora et al.,<sup>8</sup> large eddy simulations of Nichols et al.<sup>15,16</sup> and with analyses by Gee et al.<sup>20</sup> for solid rocket motor noise.

Although the spatial trends are similar, Fig. 5(c) depicts a dramatic increase in  $Sk\{\partial p/\partial t\}$  for 150% ETR relative to 50% ETR, with values of 3.3–4.1 near the shear layer and a maximum value exceeding 12 near the peak radiation direction. This figure provides significant insight into the nature of the radiation of finite-amplitude noise from military jet aircraft, with the F-35 engine being the most powerful tactical aircraft engine built. Whereas there is broad spatial region with relatively constant pressure skewness, the derivative skewness grows rapidly with increasing distance. The region of large derivative skewness stems from the maximum source region near the shear layer toward the maximum OASPL direction (~110–140°) in Fig. 5(a). Quantitatively, the derivative skewness values are consistent with steepened waveforms near the jet shear layer and shock formation by 38 m, which is confirmed by visual inspection of waveforms in Ref. 40. A previous investigation<sup>34</sup> with 100% ETR suggested that the apparent derivative skewness origin was upstream of the maximum OASPL origin, but this does not appear to be the case for afterburner, thus requiring further investigation. The derivative skewness also increases with distance in the sideline and forward directions, reaching greater values than in the aft direction for 50% ETR, which suggests nonlinear steepening occurs in the forward direction at afterburner.

Some additional comments and analyses regarding spatial trends for both pressure and derivative skewness are worthwhile. First, Figs. 4(b) and 5(b) do not indicate strong propagation trends for  $Sk\{p(t)\}$ , again pointing to waveform asymmetry as a source phenomenon that increases with engine power. However, a decrease in positive  $Sk\{p(t)\}$  will occur in the far field for two reasons. First, weak atmospheric dispersion will produce a slight rounding of positive waveform peaks. Second, large pressure outliers will be suppressed due to nonlinear propagation losses. Consequently, the effect of far-field propagation is to eventually create essentially Gaussian-distributed pressure amplitudes, similar to the far-field static run-up F-22 data noted by Gee and Sparrow<sup>48</sup> and flyover data by McInerny et al.<sup>19</sup>. It is also important to note that many of the skewness values in Fig. 5(b) for the F-35 AA-1 at 150% ETR would be considered borderline by the traditional Ffowcs Williams et al.<sup>1</sup> crackle criterion. Despite the qualitative nature of Ffowcs Williams et al.'s description of “distinctly crackling,” there is no question that crackle is readily audible in sideline and downstream noise from the F-35 AA-1 at afterburner power. Thus, Fig. 5(b) provides clear evidence beyond the caution by Papamoschou and Debiasi<sup>4</sup> and by Gee et al.<sup>23</sup> that pressure skewness, and in particular the Ffowcs Williams et al. criterion, are inadequate quantifiers of crackle.

Although the pressure PDF should become more Gaussian in the far field, resulting in negligible pressure skewness, the evolution of the pressure derivatives is controlled by the relative importance of the nonlinear propagation. The near shear-layer minimum and 38-m maximum derivative skewness values are summarized in Table 1 as a function of engine condition from 25 to 150% ETR. Spatial plots, similar to Figs. 4(c) and 5(c) but without the bicubic regularization, were shown for additional engine powers in

*Table 1—Summary of  $Sk\{\partial p/\partial t\}$  growth as a function of engine condition from the minimum value at the two microphones closest to the shear layer to the maximum value at 38 m across the microphones located between 90 and 150°.*

ETR (%)	$Sk\{\partial p/\partial t\}$		
	Near shear-layer min	38m, 90–150 max	Percentage increase
25	$2.80e-03$	0.070	2380%
50	0.161	1.62	909%
75	0.709	10.2	1340%
100	1.36	8.71	540%
130	3.00	9.65	221%
150	3.34	11.0	228%

Ref. 40. The near-shear-layer minimum values for  $Sk\{\partial p/\partial t\}$  monotonically increase with engine condition, signifying greater nonlinear waveform steepening near the source. The values for all conditions, however, are below the suggested threshold for significant shock formation. At 38 m, 50% ETR serves as an intermediate case between essentially no nonlinear propagation (25% ETR) to significant shock formation (75% ETR). In addition to Ref. 40, visual evidence of shock formation was shown in Ref. 34, which contained waveforms for 100% ETR (military power). At this condition,  $Sk\{\partial p/\partial t\}$  increases from  $\sim 1.36$  near the shear layer to a maximum greater than 8.7 at 38 m. Examination of an amplitude-normalized, retarded time-aligned waveform segment along  $130^\circ$  at 8 and 38 m revealed that while both waveforms were skewed, only the 38 m waveform had significant shock content.

Table 1 reveals a large change in sound field characteristics that occurs somewhere between 50 and 75% ETR. Although the jet fluid mechanics related to this change are presently unknown, there is an approximate 10 dB increase in maximum OASPL at the 38 m arc between the two conditions, which is apparently enough to increase nonlinear propagation to the point of shock formation. The reason that the maximum derivative skewness at 38 m for 100 and 130% ETR decreases slightly relative to 75% ETR is not clear, because both the overall sound levels and the near shear-layer derivative skewness are both increasing, as well as the overall angular aperture of significant

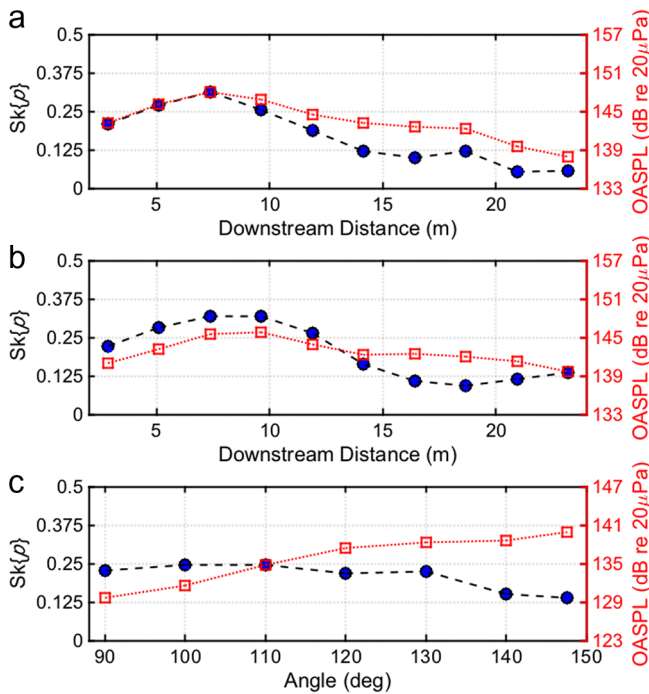


Fig. 6—OASPL and  $Sk\{p(t)\}$  at (a) Plane 1, (b) Plane 2 and (c) The 23-m arc, averaged over the top 18 array microphones for the F-22 Raptor military power.

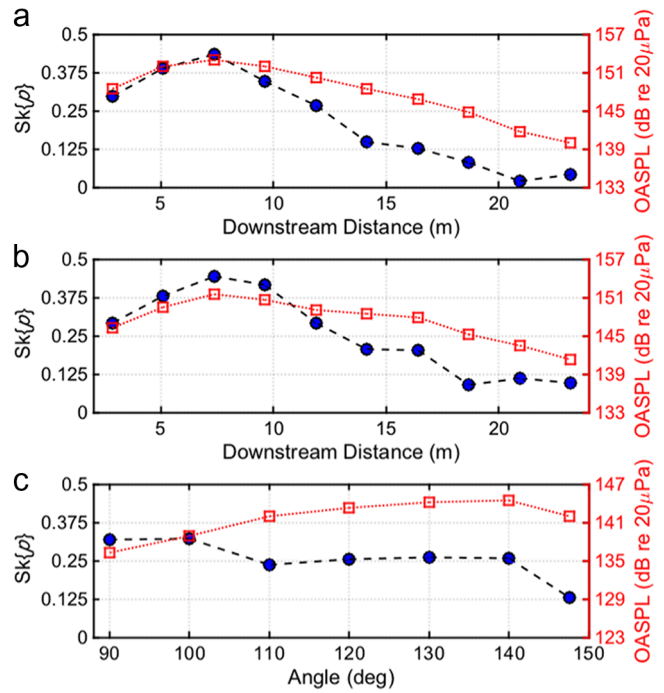


Fig. 7—OASPL and  $Sk\{p(t)\}$  at (a) Plane 1, (b) Plane 2 and (c) The 23-m arc, averaged over the 18 microphones at nozzle height for the F-22 Raptor afterburner power.

derivative skewness<sup>40</sup>. In any event, when contrasted with the relatively constant pressure skewness values, the growth in derivative skewness for 75% and greater ETR demonstrates the significant phenomenological differences in the proposed definitions for jet crackle and its treatment as a source versus propagation phenomenon.

## 5 F-22A DATA ANALYSIS

### 5.1 Spatial and Engine Condition Comparison

The OASPL,  $Sk\{p(t)\}$  and  $Sk\{\partial p/\partial t\}$  near the F-22A Raptor for military and afterburner powers corroborate the source versus propagation characteristics of the radiated field shown in Sec. 4. Data are conveniently represented by spatially averaging calculations from the row of microphones at the engine centerline height (see Figs. 2 and 3) to produce a single average for each rectangular array position. The averaged metrics are shown along plane 1, plane 2 and the 23-m arc for military and afterburner conditions in Figs. 6–9. Figures 6 and 7 show the OASPL and pressure skewness results for military and afterburner powers, respectively, and Figs. 8 and 9 contain the OASPL and derivative skewness results for both engine conditions. Because the afterburner engine condition was measured at a lower sampling frequency than military conditions (48 kHz vs. 96 kHz), a discussion of the effect of the

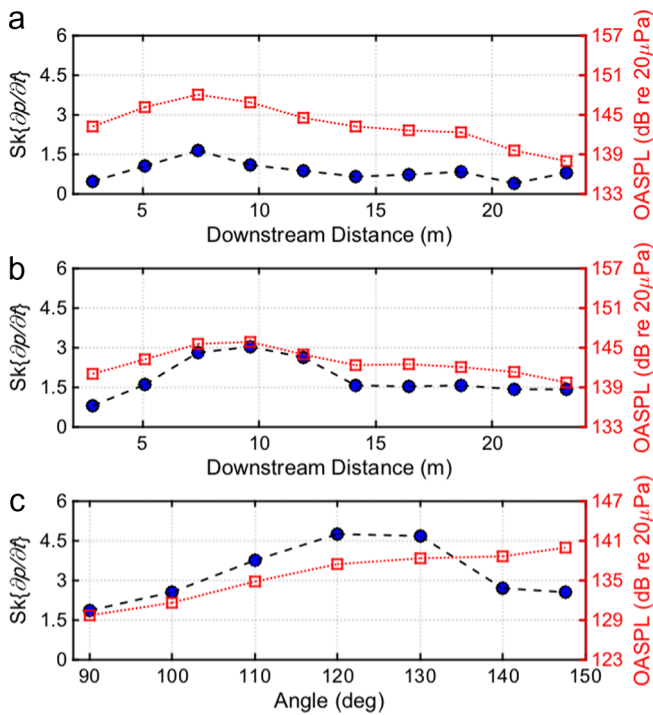


Fig. 8—OASPL and  $Sk\{\partial p/\partial t\}$  at (a) Plane 1, (b) Plane 2 and (c) The 23-m arc, averaged over the 18 microphones at nozzle height for the F-22 Raptor at military power.

sampling frequency on skewness estimation using the F-22A data is also presented.

In Figs. 6 and 7, the maximum OASPL for both engine conditions along plane 1 reaches a maximum of 148 dB for military condition and 153 dB for afterburner at approximately 7–8 m downstream of the nozzle. For  $Sk\{p(t)\}$ , the spatial trend is similar to the OASPL along planes 1 and 2 in that both quantities reach their maxima in similar regions and decrease with downstream distance. However, at the 23 m arc, the maximum values of  $Sk\{p(t)\}$  occur appreciably upstream of the maximum OASPL region in Figs. 6(c) and 7(c) and do not increase with distance, which corroborates the F-35 analysis in Sec. 4. For military power in Fig. 6, the range of maximum  $Sk\{p(t)\}$  falls between 0.25 and 0.4. For the afterburner data,  $Sk\{p(t)\}$  approaches 0.5 along planes 1 and 2, but decreases by the 23 m arc to values of 0.35. Again, the values at 23 m would be only “marginally” crackling according to the Ffowcs Williams et al. criterion, which disagrees with field observations.

Values of  $Sk\{\partial p/\partial t\}$  for the F-22A at military power in Fig. 8 show similar behavior as the F-35 AA-1. The maximum in Fig. 8(b) along plane 1 is approximately 1.5 and increases to 4.7 at 23 m. Comparison with the F-35 AA-1: Fig. 5(c) at afterburner and Fig. 2(b) in Ref. 34 for 100% ETR in the maximum radiation direction reveals values that range between 2.5 and 6.2 over comparable distances. The trend of systematic, significant

growth of nonlinear steepening away from the shear layer through plane 1, plane 2 and the arc is unmistakable.

Because the rate of nonlinear waveform steepening is expected to increase with OASPL, comparison of Figs. 8 and 9 for the F-22A at military and afterburner conditions reveals an initially counterintuitive trend —  $Sk\{\partial p/\partial t\}$  starts out larger for afterburner along plane 1 but then grows more slowly, such that the maximum value on the arc is 3.1 versus 4.7 obtained for military power. It was noted previously that the afterburner data were acquired at a lower sampling rate and, as indicated in Ref. 31 and Sec. 5.1, sampling rate plays a key role in determining derivative skewness estimates as shocks begin to form. Thus, an examination of the relationship between sampling rate and derivative skewness using F-22A military-power noise waveforms is worthwhile.

## 5.2 Impact of Sampling Frequency on $Sk\{\partial p/\partial t\}$

In addition to analytical investigations<sup>31,32</sup>, the dependence of  $Sk\{\partial p/\partial t\}$  on sampling rate has been briefly discussed by Gee et al.<sup>9</sup> in analysis of supersonic, laboratory-scale data. For the laboratory-scale jet, the values of  $Sk\{\partial p/\partial t\}$  were significantly less than for the F-35 AA-1 in Refs. 34 and 40 and in Fig. 5(c), yet visual inspection of the waveform showed it contained significant shocks. To evaluate this apparent contradiction, it is therefore

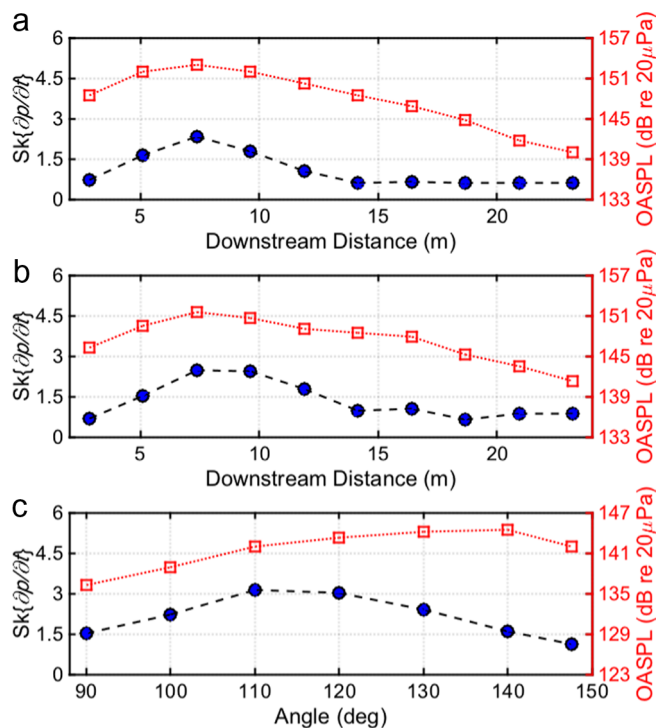


Fig. 9—OASPL and  $Sk\{\partial p/\partial t\}$  at (a) Plane 1, (b) Plane 2 and (c) The 23-m arc, averaged over the 18 microphones at nozzle height for the F-22 Raptor at afterburner power.

useful to analyze the effect of sampling rate on the calculation of  $Sk\{p(t)\}$  and  $Sk\{\partial p/\partial t\}$  for the F-22A at military power by numerically downsampling the waveforms of the military power measurement prior to statistical calculations.

Figure 10 shows  $Sk\{p(t)\}$  and  $Sk\{\partial p/\partial t\}$  as a function of the ratio between sampling frequency and spectral peak frequency,  $f_s/f_{peak}$ , at three locations on the arc at 23 m, 90°, 120° and 150° (see Fig. 3 for definitions of these angles). Below a certain  $f_s/f_{peak}$  threshold, the skewness estimates at any angle become random and meaningless, but the threshold is location-dependent. Above the  $f_s/f_{peak}$  threshold, the estimates for both quantities steadily increase. For the case of  $Sk\{p(t)\}$  in Fig. 10(a), it appears that the skewness estimates reach asymptotic values at all locations as  $f_s/f_{peak}$  increases. The ratio at which the asymptotic value is reached varies with location, likely due to the spatial variation in the spectrum<sup>42</sup> and indicates the frequency ratio that is, or is nearly, sufficient to estimate the true pressure skewness. The results also suggest that for some locations, including near the maximum radiation direction, the sampling frequency must be a factor of 100 greater than the peak frequency for accurate calculations of  $Sk\{p(t)\}$ . Thus, because the peak frequency for the F-22 at afterburner is less than 500 Hz, the

sampling frequency of only 48 kHz is likely sufficient to accurately estimate the  $Sk\{p(t)\}$  in Fig. 7. This rule-of-thumb,  $f_s/f_{peak} > 100$ , might be used to assess data sufficiency in laboratory-scale experiments for characterizing  $Sk\{p(t)\}$ .

A different scenario exists for the dependence of  $Sk\{\partial p/\partial t\}$  on  $f_s/f_{peak}$ , as shown in Fig. 10(b). Above  $f_s/f_{peak} \approx 5$ , the estimates for the three different angles all increase with  $f_s/f_{peak}$  but, unlike  $Sk\{p(t)\}$ , the values for  $Sk\{\partial p/\partial t\}$  do not plateau, even for the maximum  $f_s/f_{peak}$  represented by the 96 kHz sampling rate. Since shocks in a lossy medium are, in fact, continuous functions with finite thickness, we presume that the derivative skewness values will not approach infinity with increasing sampling rate, but will rather approach an asymptotic value for greater values of  $f_s/f_{peak}$ . However, because a positive slope persists at the maximum value of  $f_s/f_{peak}$  for each curve in Fig. 10(b), a sampling frequency of 96 kHz is insufficient to accurately capture the actual shock rise times for full-scale engine data. The variation in slope along each curve in Fig. 10(b) is likely caused by the inclusion or exclusion of ground-reflected shocks in the waveform, which depends on experiment geometry and  $f_s/f_{peak}$ . Although the presence of a reflecting plane does not change the principal conclusions of this paper, additional investigations that examine these statistical measures as a function of microphone height above a reflecting surface would provide additional physical insight about the propagation of high-performance jet noise as it relates to personnel noise environments.

In addition to illustrating the need for high sampling rates, Fig. 10(b) also illustrates the problem of making comparable laboratory measurements where scaled measurement bandwidths are not possible. As an example of the potential utility of Fig. 10 in helping to assess differences between laboratory and full-scale measurements, we compare the nominal  $f_s/f_{peak}$  for an unheated Mach 2.0 jet in Ref. 9 with the F-35 AA-1 in the maximum derivative skewness direction. The maximum  $Sk\{\partial p/\partial t\}$  in Table 1 for 100% ETR is 8.71; at the same scaled location for the laboratory measurement,  $Sk\{\partial p/\partial t\}$  was approximately 2.4, a ~73% reduction in skewness. For the F-35 AA-1 at military power,  $f_s/f_{peak} \approx 450$ , whereas for the laboratory-scale jet (sampled at 192 kHz),  $f_s/f_{peak} \approx 70$ . A comparison of the derivative skewness corresponding with those two frequency ratios on the 120° and 150° curves in Fig. 10(b) suggests a reduction of ~50–75% in  $Sk\{\partial p/\partial t\}$ , purely by sampling considerations without counting differences in shock strength due to source or propagation medium differences. The observed 73% reduction in  $Sk\{\partial p/\partial t\}$  falls within these bounds.

To return to the original goal of making a more accurate quantitative comparison between military and afterburner conditions for the F-22A measurements, reduction of the

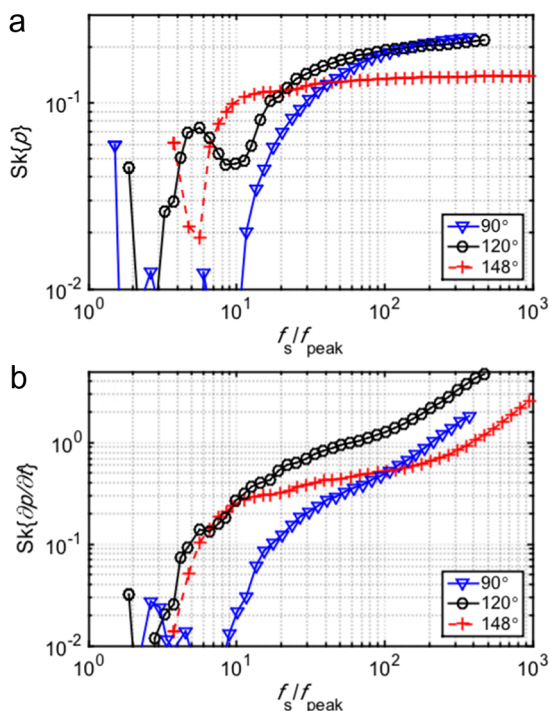


Fig. 10—(a)  $Sk\{p(t)\}$  and (b)  $Sk\{\partial p/\partial t\}$  as a function of  $f_s/f_{peak}$  at 90°, 120° and 150° for the F-22A experiment along the 23 m arc for the F-22 Raptor at military power.

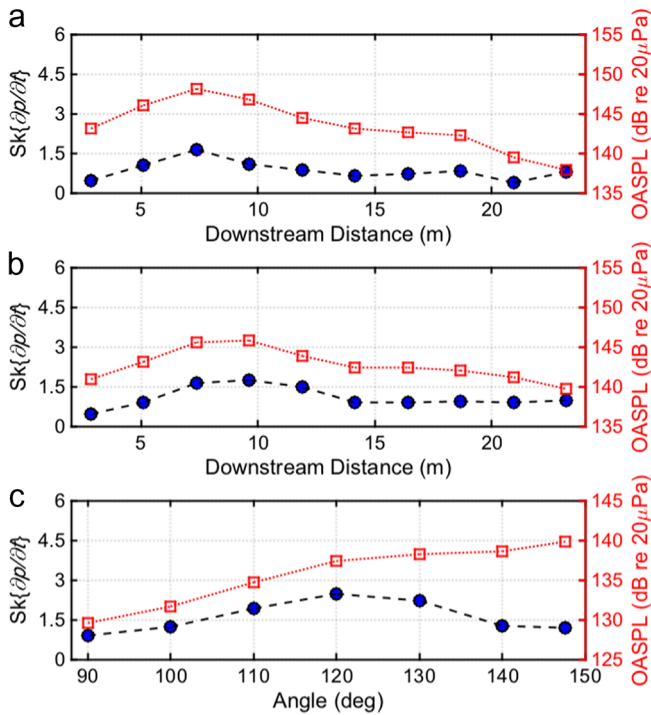


Fig. 11— $Sk\{\partial p/\partial t\}$  for downsampled (96 kHz to 48 kHz) military power data shown previously in Fig. 8.

sampling rate by a factor of two in Fig. 10 reveals only marginal changes in  $Sk\{p(t)\}$ , but much larger changes (approaching a factor of 1.5) in  $Sk\{\partial p/\partial t\}$ . The derivative skewness resulting from downsampling is shown in Fig. 11. The comparison between  $Sk\{\partial p/\partial t\}$  in Figs. 9 (for afterburner) and 11 (downsampled military case) reveals what was anticipated on physical grounds previously — the maximum  $Sk\{\partial p/\partial t\}$  for the downsampled military data is 2.6, which is less than the 3.1 for afterburner. If an extrapolation of the afterburner data in the form of a doubling of sampling frequency is allowed, Fig. 10(b) suggests that the maximum value of  $Sk\{\partial p/\partial t\}$  will increase from 3.1 to 4.7. This is consistent with a derivative skewness value of 4.8 reported for an afterburning F-22A at 23 m and 125°<sup>49</sup>. When sampling rate is taken into account, these findings from the F-22A dataset emphasize the range and amplitude-dependent evolution of  $Sk\{\partial p/\partial t\}$  in high-amplitude jet noise, thus corroborating the F-35 AA-1 investigation.

## 6 CONCLUDING DISCUSSION

From the present investigation, we conclude that the historical definition of jet crackle synonymous with pressure waveform skewness greater than 0.4 is phenomenologically different from a definition of crackle that is based on the presence of acoustic shocks. Skewed pressure waveforms can be readily described as a source phenomenon for supersonic jets, based on these full-scale data and

prior laboratory measurements and numerical simulations. However, based on the waveform analysis of both the F-35 AA-1 and F-22A datasets using the skewness of the pressure derivative, we find that nonlinear acoustic propagation for high engine powers causes the skewed, steepened waveforms that exist near the shear layer to undergo further waveform steepening and eventually form a significant number of shocks. Furthermore, these shocks evolve and persist well into the geometric far field, even for cases where the pressure skewness becomes negligible<sup>48</sup>. The full-scale analyses here are complemented by laboratory-scale studies<sup>8,9</sup> that have also shown a significant increase in derivative statistics with propagation distance.

Thus, a definition of jet crackle that is quantitatively based on a measure sensitive to shock formation needs to be couched within the understanding that the phenomenon is heavily influenced by nonlinear acoustic propagation. We believe that this framework will ultimately provide a greater link between physical and perceptual characteristics of crackle. This is not to say that positive pressure skewness is not an important source feature unique to supersonic jets, only that it is not a quantifier of the crackle phenomenon.

We should point out that Ffowcs Williams et al. considered, but rejected, the notion that *cumulative* nonlinear propagation effects (i.e., those that continue to evolve the waveform beyond the source's acoustic near field) influenced the presence of the acoustic shocks in the data. They surmised (incorrectly, based on then-concurrent<sup>50,51</sup> and more recent<sup>6,12,19,35–37,52</sup> investigations) that nonlinear distortion of waveforms in the far field of supersonic jet noise is negligible and, therefore, the nonlinearity and resultant rapid pressure changes must occur at the source. Other recent studies have supported the idea that the acoustic shocks are source-related<sup>15,16</sup> or are due to other near-field nonlinear phenomena<sup>26,27,29</sup> and not nonlinear waveform steepening. However, per the sampling rate issues considered here, the influence of a limited experiment or numerical simulation bandwidth on their conclusions is unknown and it is possible that our view that “steepened” waveforms exist near the source and others' views that “shocks” exist near the source are entirely compatible.

This investigation points to the need for additional work related to crackle. First, coupling of high-fidelity measurements and simulations is needed<sup>15–17</sup>. Second, sampling-rate and ground reflection-related investigations need to be carried out to better represent measurement realities. Finally, this analysis points to a further need to understand crackle as a perceptual phenomenon because of recent efforts tying crackle to jet noise reduction<sup>7,8,14</sup>. If perception is linked to the prevalence and steepness of the acoustic shocks, we believe that the crackle percept will be more pronounced farther from the jet, despite geometric-spreading-induced reductions

in overall level. Consequently, we caution that jet engine noise reduction measures that target a lessening of pressure skewness in an attempt to reduce crackle, without effecting a significant change in overall level, may not function as anticipated. Nonlinear propagation resulting in shock formation away from the jet exhaust could still produce strong crackle-like perception.

## 7 ACKNOWLEDGMENTS

The authors gratefully acknowledge funding from the Air Force SBIR program and the Office of Naval Research Jet Noise Reduction program to complete these analyses. The measurements were funded by the Air Force Research Laboratory through a prior SBIR program<sup>2)</sup> and supported through a Cooperative Research and Development Agreement (CRDA) between Blue Ridge Research and Consulting LLC, Brigham Young University and the Air Force. Distribution A — approved for public release; distribution is unlimited; JSF clearance numbers JSF 13-450 and JSF14-592 and USAF clearance number 88ABW-2013-2296.

## 8 REFERENCES

1. J.E. Ffowcs Williams, J. Simson and V.J. Virchis, “‘Crackle’: An annoying component of jet noise”, *J. Fluid Mechanics*, **71**, 251–271, (1975).
2. A. Krothapalli, L. Venkatakrishnan and L. Lourenco, “Crackle: A dominant component of supersonic jet mixing noise”, AIAA paper No. 2000-2024, (2000).
3. R.H. Schlinker, “Supersonic jet noise experiments”, Ph.D. dissertation, Dept. of Aerospace Engineering, Univ. Southern California, (1975).
4. D. Papamoschou and M. Debiasi, “Directional suppression of noise from a high-speed jet”, *AIAA J.*, **39**, 380–387, (2001).
5. B.P. Petitjean and D.K. McLaughlin, “Experiments on the nonlinear propagation of noise from supersonic jets”, AIAA paper No. 2003-3127, (2003).
6. B.P. Petitjean, K. Viswanathan and D.K. McLaughlin, “Acoustic pressure waveforms measured in high speed jet noise experiencing nonlinear propagation”, *Int. J. Aeroacoustics*, **5**, 193–215, (2006).
7. S. Martens, J.T. Spyropoulos and Z. Nagel, “The effect of chevrons on crackle — Engine and scale model results”, *ASME Turbo Expo 2011*, (2011).
8. P. Mora, N. Heeb, J. Kastner, E.J. Gutmark and K. Kailasanath, “Effect of heat on the pressure skewness and kurtosis in supersonic jets”, *AIAA J.*, **52**, 777–787, (2014).
9. K.L. Gee, T.B. Neilsen and A.A. Atchley, “Skewness and shock formation in laboratory-scale supersonic jet data”, *J. Acoust. Soc. Am.*, **133**, EL491–EL497, (2013).
10. R.H. Schlinker, S.A. Liljenberg, D.R. Polak, K.A. Post, C.T. Chipman and A.M. Stern, “Supersonic jet noise source characteristics and propagation: Engine and model scale”, AIAA paper No. 2007-3623, (2007).
11. R.H. Schlinker, J.C. Simonich, R.A. Reba, T. Colonius and F. Ladeinde, “Decomposition of high speed jet noise: Source characteristics and propagation effects”, AIAA paper No. 2008-2890, (2008).
12. S.A. McNerny, M. Downing, C. Hobbs and M. Hannon, “Metrics that characterize nonlinearity in jet noise”, *Innovations in Nonlinear Acoustics (ISNA 17)*, AIP Conference Proceedings, **838**, 560–563, (2006).
13. D.G. Crighton, “Nonlinear acoustic propagation of broadband noise”, *Recent Advances in Aeroacoustics*, Springer-Verlag, New York, (1986), pp. 411–454.
14. A. Krothapalli, B. Greska and V. Arakeri, “High-speed jet noise reduction using microjets”, Chap. 3 in *Combustion Processes in Propulsion: Control, Noise, and Pulse Detonation*, edited by G. D. Roy, Elsevier, Burlington, MA, (2006).
15. J.W. Nichols, S.K. Lele, F.E. Ham, S. Martens and J.T. Spyropoulos, “Crackle noise in heated supersonic jets”, *J. Eng. Gas Turbines and Power*, **135**(5), 051202–051202-7, (2013).
16. J.W. Nichols, S.K. Lele and J.T. Spyropoulos, “The source of crackle noise in heated supersonic jets”, AIAA paper No. 2013-2197, (2013).
17. A.T. Anderson and J.B. Freund, “Source mechanisms of jet crackle”, AIAA paper No. 2012-2251, (2012).
18. D.A. Buchta, A.T. Anderson and J.B. Freund, “Near-field shocks radiated by high-speed free-shear-flow turbulence”, AIAA paper No. 2014-3201, (2014).
19. S.A. McNerny, K.L. Gee, J.M. Downing and M.M. James, “Acoustical nonlinearities in aircraft flyover data”, AIAA paper No. 2007-3654, (2007).
20. K.L. Gee, R.J. Kenny, T.B. Neilsen, T.W. Jerome, C.M. Hobbs and M.M. James, “Spectral and statistical analysis of noise from reusable solid rocket motors”, *Mtgs. Acoust.*, **18**, 040002, (2013).
21. S.A. McNerny, “Launch vehicle acoustics part 2: Statistics of the time domain data”, *J. Aircraft*, **33**, 518–523, (1996).
22. D. Fee, R.S. Matoza, K.L. Gee, T.B. Neilsen and D.E. Ogden, “Infrasonic crackle and supersonic jet noise from the eruption of Nabro Volcano”, *Geophys. Res. Letters*, **40**, 2780–2785, (2013).
23. K.L. Gee, V.W. Sparrow, A.A. Atchley and T.B. Gabrielson, “On the perception of crackle in high-amplitude jet noise”, *AIAA J.*, **45**, 593–598, (2007).
24. S.H. Swift and K.L. Gee, “Examining the use of a time-varying loudness algorithm for quantifying characteristics of nonlinearly propagated noise”, *J. Acoust. Soc. Am.*, **129**, 2753–2756, (2011).
25. W.J. Baars and C.E. Tinney, “Shock structures in the acoustic field of a Mach 3 jet with crackle”, *J. Sound Vibr.*, **333**, 2539–2553, (2014).
26. S.A. McNerny, J.K. Francine, B.S. Stewart and P.H. Thorson, “The influence of low-frequency instrumentation response on rocket noise metrics”, *J. Acoust. Soc. Am.*, **102**, 2780–2785, (1997).
27. W.J. Baars, C.E. Tinney, M.S. Wochner and M.F. Hamilton, “On cumulative nonlinear acoustic waveform distortions from high-speed jets”, *J. Fluid Mech.*, **749**, 331–366, (2014).
28. R.W. Powers, D.K. McLaughlin, P.J. Morris and C.-W. Kuo, “Supersonic jet noise reduction by nozzle fluidic inserts with simulated forward flight”, AIAA paper No. 2014-2474, (2014).

<sup>2)</sup> SBIR DATA RIGHTS - (DFARS 252.227-7018 (JUNE 1995)); Contract Number: FA8650-08-C-6843; Contractor Name & Address: Blue Ridge Research and Consulting, LLC, 15 W Walnut St., Suite C; Asheville, NC. Expiration of SBIR Data Rights Period: March 17, 2016 (Subject to SBA SBIR Directive of September 24, 2002.). The Government's rights to use, modify, reproduce, release, perform, display, or disclose technical data or computer software marked with this legend are restricted during the period shown as provided in paragraph (b)(4) of the Rights in Noncommercial Technical Data and Computer Software—Small Business Innovation Research (SBIR) Program clause contained in the above identified contract. No restrictions apply after the expiration date shown above. Any reproduction of technical data, computer software, or portions thereof marked with this legend must also reproduce the markings.

29. R. Fiévet, C.E. Tinney and W.J. Baars, “Acoustic waveforms produced by a laboratory scale supersonic jet”, AIAA paper No. 2014-2906, (2014).
30. M.R. Shepherd, K.L. Gee and A.D. Hanford, “Evolution of statistics for a nonlinearly propagating sinusoid”, *J. Acoust. Soc. Am.*, **130**, EL8–EL13, (2011).
31. B.O. Reichman, M.B. Muhlestein, K.L. Gee, T.B. Neilsen and D.C. Thomas, “Evolution of the pressure derivative skewness for nonlinearly propagating waves”, submitted to *J. Acoust. Soc. Am.*, (2014).
32. M.B. Muhlestein, “Analyses of nonlinearity measures in high-amplitude sound propagation”, M.S. thesis, Dept. of Physics and Astronomy, Brigham Young University, (2013).
33. M.B. Muhlestein and K.L. Gee, “Experimental investigation of a characteristic shock formation distance in finite-amplitude noise propagation”, *Mtgs. Acoust.* **12**, 045002, (2011).
34. K.L. Gee, T.B. Neilsen, J.M. Downing, M.M. James, R.L. McKinley, R.C. McKinley and A.T. Wall, “Near-field shock formation in noise propagation from a high-power jet aircraft”, *J. Acoust. Soc. Am.*, **133**, EL88–EL93, (2013).
35. R. McKinley, R. McKinley, K.L. Gee, T. Pilon, F. Mobley, M. Gillespie and J.M. Downing, “Measurement of near-field and far-field noise from full scale high performance jet engines”, *ASME Turbo Expo 2010*, (2010).
36. K.L. Gee, J.M. Downing, M.M. James, R.L. McKinley, R.C. McKinley, T.B. Neilsen and A.T. Wall, “Nonlinear evolution of noise from a military jet aircraft during ground run-up”, AIAA paper No. 2012-2258, (2012).
37. K.L. Gee, V.W. Sparrow, M.M. James, J.M. Downing, J.M. Hobbs, T.M. Gabrielson, T.B. Neilsen and A.A. Atchley, “The role of nonlinear effects in the propagation of noise from high-power jet aircraft”, *J. Acoust. Soc. Am.*, **123**, 4082–4093, (2008).
38. K.L. Gee, T.B. Neilsen and M.M. James, “On the crest factor of noise in full-scale supersonic jet engine measurements”, *Mtgs. Acoust.*, **20**, 045003, (2013)
39. T.B. Neilsen, K.L. Gee, A.T. Wall, M.M. James and A.A. Atchley, “Comparison of supersonic full-scale and laboratory-scale jet data and the similarity spectra for turbulent mixing noise”, *Mtgs. Acoust.*, **19**, 040071, (2013).
40. K.L. Gee, T.B. Neilsen, B.O. Reichman, M.B. Muhlestein, D.C. Thomas, J.M. Downing, M.M. James and R.L. McKinley, “Comparison of two time-domain measures of nonlinearity in near-field propagation of high-power jet noise”, AIAA Paper No. 2014-3199, (2014).
41. A.T. Wall, K.L. Gee, M.M. James, K.A. Bradley, S.A. McNerny and T.B. Neilsen, “Near-field noise measurements of a high-power jet aircraft”, *Noise Control Engr. J.*, **60**, 421–434, (2012)
42. T.B. Neilsen, K.L. Gee, A.T. Wall and M.M. James, “Similarity spectra analysis of high-performance jet aircraft noise”, *J. Acoust. Soc. Am.*, **133**, 2116–2125, (2013).
43. B.M. Harker, K.L. Gee, T.B. Neilsen, A.T. Wall, S.A. McNerny and M.M. James, “On autocorrelation analysis of jet noise”, *J. Acoust. Soc. Am.*, **133**, EL458–EL464, (2013).
44. T.A. Stout, K.L. Gee, T.B. Neilsen, A.T. Wall and M.M. James, “Acoustic intensity near a high-power military jet aircraft”, *J. Acoust. Soc. Am.*, **138**, EL1–EL7, (2015).
45. A.T. Wall, K.L. Gee, T.B. Neilsen, D.W. Krueger and M.M. James, “Cylindrical acoustical holography applied to full-scale jet noise”, *J. Acoust. Soc. Am.*, **136**, 1120–1128, (2014).
46. J. Morgan, T.B. Neilsen, K.L. Gee, A.T. Wall and M.M. James, “Simple-source model of high-power jet aircraft noise”, *Noise Control Engr. J.*, **60**, 435–449, (2012)
47. <http://www.mathworks.com/matlabcentral/fileexchange/46223-regularizedata3d>. Last accessed 18 July 2014.
48. K.L. Gee and V.W. Sparrow, “Quantifying nonlinearity in the propagation of noise from military jet aircraft”, *NoiseCon05*, (2005).
49. K.L. Gee, “Prediction of nonlinear jet noise propagation”, Ph.D. thesis, The Pennsylvania State University, (2005).
50. D.T. Blackstock, “Nonlinear propagation of jet noise”, *Third Interagency Symp. on University Research in Transportation Noise*, (1975).
51. D.A. Webster and D.T. Blackstock, “Experimental investigation of outdoor propagation of finite-amplitude noise”, NASA Contractor Report 2992. Applied Research Laboratories, The University of Texas at Austin, (1978).
52. B. Greska and A. Krothapalli, “On the far-field propagation of high-speed jet noise”, *NCAD2008*, Paper NCAD2008-73071, (2008).